**Table 2 Dimensionless time constant of vortex breakdown recovering from the instant of blowing cessation**

| AOA, deg | | Periodic blowing, $\tau^* = \tau U_\infty / C$ | | | |
|---|---|---|---|---|---|
| | | $f_r = 1.25$ | $f_r = 2.5$ | $f_r = 3.75$ | $f_r = 5.0$ |
| $\alpha = 45$ | $C_\mu = 0.06$ | 2.52 | 1.86 | 1.28 | 0.84 |
| $\alpha = 45$ | $C_\mu = 0.088$ | 3.04 | 2.56 | 2.16 | 1.68 |
| $\alpha = 40$ | $C_\mu = 0.06$ | 3.2 | 2.44 | 1.72 | 0.96 |

## Acknowledgment

The authors are grateful for the support of this investigation from the National Science Foundation of Republic of China under Grant NSC-82-0618-E-005-096.

## References

[1]Tavella, D., "Lift of Delta Wings with Leading Edge Blowing," *Journal of Aircraft*, Vol. 25, No. 6, 1987, pp. 522–524.

[2]Wood, N. J., and Robert, L., "Control of Vortical Lift on Delta Wings by Tangential Leading Edge Blowing," *Journal of Aircraft*, Vol. 25, No. 3, 1987, pp. 236–243.

[3]Bradley, R. G., Whitten, P. D., and Wray, W. O., "Leading-Edge Vortex Augmentation in Compressible Flow," *Journal of Aircraft*, Vol. 13, No. 9, 1976, pp. 238–242.

[4]Campbell, J. F., "Augmentation of Vortex Lift by Spanwise Blowing," *Journal of Aircraft*, Vol. 13, No. 9, 1976, pp. 727–732.

[5]Shi, Z., Wu, J. M., and Vakili, A. D., "An Investigation of Leading-Edge Vortices on Delta Wing With Jet Blowing," AIAA Paper 87-0330, Jan. 1987.

[6]Visser, K. D., Iwanski, K. T., Nelson, R. C., and Ng, T. T., "Control of Leading-Edge Vortex Breakdown By Blowing," AIAA Paper 88-0504, Jan. 1988.

[7]Parmenter, K., and Rockwell, D., "Transient Response of Leading Edge Vortices to Localized Suction," *AIAA Journal*, Vol. 28, No. 6, 1990, pp. 1131–1133.

# Conjugate Gradient Squared Algorithm for Panel Methods

Santhosh P. Koruthu*
*Aeronautical Development Agency, Bangalore 560 017, India*

## Introduction

PANEL methods are the most efficient of numerical schemes to obtain solutions to linear potential flow problems. The efficiency of these methods arises primarily from the fact that, in a panel method, the effective dimensionality of the problem is one less than the spatial dimension of the flowfield. This is because the problem of solving the governing partial differential equation for the field is transformed into an equivalent problem of solving an integral equation for the surface. Panel methods solve this integral equation numerically. The efficiency of these methods makes them useful tools in tradeoff studies in aircraft design.

Numerical solution of the integral equation using a panel method gives rise to fully populated linear systems, in general. This is in contrast with the finite difference, finite element, and finite volume techniques employed in computational fluid dynamics where each linearized step in the solution algorithm gives rise to a sparse linear system. When the flow past a complicated configuration is analyzed using a panel method, it is difficult to ensure any specific structure to the matrix of the linear system. Often, diagonal dominance cannot be assured. Therefore, when solving such systems, most classical iterative schemes are slow in convergence. Many panel codes use Gaussian elimination [lower-upper (LU) decomposition] as an alternative.[1] This requires $\mathcal{O}(n^3)$ floating point operations where $n$ is the order of the matrix. An iterative scheme requires only $\mathcal{O}(n^2)$ floating point operations. Therefore it is desirable to have robust iterative schemes, especially for situations where the order of the matrix is large, such as would be the case when analyzing flow past complex configurations.

A variety of conjugate gradient type methods have evolved as potential linear system solvers. The conjugate gradient squared (CGS) method is one that has been proposed for nonsymmetric and nonpositive definite systems.[2] The present paper examines the use of this scheme for systems of linear algebraic equations encountered in panel methods.

## Present Panel Method

A low-order panel method for subcritical flows has been used in the present study. The governing flow equation is the Prandtl–Glauert equation for the velocity potential $\phi$:

$$\left(1 - M_\infty^2\right)\phi_{xx} + \phi_{yy} + \phi_{zz} = 0 \tag{1}$$

Here subscripts denote partial differentiation; $M_\infty$ is the freestream Mach number. Using a stretching transformation, this equation is reduced to the Laplace equation:

$$\phi_{xx} + \phi_{yy} + \phi_{zz} = 0 \tag{2}$$

The Laplace equation is transformed into an integral equation using Green's theorem. For a point $P$,

$$4\pi\phi(P) = \int_S [\phi] G_1 \, \mathrm{d}S + \int_S [\mathrm{grad}\,\phi \cdot \hat{n}] G_2 \, \mathrm{d}S + 4\pi\phi_\infty \tag{3}$$

The brackets [ ] refer to a jump in the enclosed quantity across the boundary $S$; $\hat{n}$ is the unit normal to surface $S$; $\phi_\infty$ is the freestream potential. It may be noted that $G_1$ is Green's function for a doublet and $G_2$ is Green's function for a source. The corresponding jump quantities in Eq. (3) can therefore be considered as doublet and source strengths. These are the unknown quantities to be determined in a panel method that solves Eq. (3) numerically.

In the present method, the source strength is prescribed a priori as the negative of the component of the freestream velocity vector normal to the surface. A Dirichlet boundary condition on the internal perturbation potential is applied to obtain the unknown doublet strength. To numerically evaluate the integrals in Eq. (3), the surface of the configuration is divided into $n$ flat panels. The centroid of each panel is chosen as the panel control point, where boundary conditions are applied. The influence (in terms of the induced velocity potential) on the control point on each panel $i$, of unit constant strength singularity distribution on each panel $j$, is calculated. For the source distributions, this influence is denoted by $B_{ij}$. For the doublet distributions, the influence is $A_{ij}$. Application of the boundary condition (of zero internal perturbation potential) at a control point $i$, using Eq. (3), gives rise to the equation

$$\sum_j A_{ij}\mu_j + \sum_j B_{ij}\sigma_j = 0 \tag{4}$$

where $\sigma_j$ and $\mu_j$ are, respectively, the source strength and the doublet strength on the $j$th panel. Since the source strengths $\sigma_j$ are prescribed, writing down Eq. (4) for each panel $i$ gives rise to a linear system

$$Ax = b \tag{5}$$

The solution of this system determines the unknown doublet strengths that uniquely determine the flowfield. Further details of the present method may be found in Ref. 3.

## CGS Algorithm and Present Implementation

Conjugate gradient (CG) algorithms are known to be very efficient for solving symmetric, positive definite linear systems. The

Received July 20, 1994; revision received Feb. 27, 1995; accepted for publication Feb. 28, 1995. 

*Project Manager, P.B. No. 1718, Vimanapura Post.

systems we consider are not of this type. The biconjugate gradient (BCG) algorithm[4] was developed as an extension of CG schemes to indefinite systems. There are some mathematically equivalent variations of this method.[5] The CGS algorithm is a generally more efficient variation of the BCG method. The CGS method has been used with success in solving the linear systems arising from unfactored implicit schemes for solving Euler and Navier–Stokes equations.[6]

The CGS method is a Krylov subspace method that, in turn, belongs to the general class of projection methods for solving linear systems. Given an initial guess $x_0$ to the linear system (5), a projection method obtains an approximate solution $x_m$ in an affine subspace $x_0 + K_m$, using the condition that the residual $b - Ax_m$ should be orthogonal to another subspace $T_m$. In a Krylov subspace method $K_m$ is chosen as a Krylov subspace defined by

$$K_m(A, r_0) = \text{span}\left(r_0, Ar_0, A^2r_0, \ldots, A^{m-1}r_0\right) \tag{6}$$

where $r_0 = b - Ax_0$. In BCG and CGS methods, the test space $T_m$ is chosen as the Krylov subspace $K_m(A^T, r_0)$. The CGS algorithm is derived in such a way that the transpose matrix $A^T$ is not required explicitly. Details of the CGS algorithm and its derivation are given in Ref. 2.

To achieve good convergence rates using CG-type schemes, it is often necessary to precondition the original system given by Eq. (5) to an equivalent system

$$M^{-1}Ax = M^{-1}b \tag{7}$$

Here $M$ is a preconditioner matrix that approximates matrix $A$. The matrix $M$ should be such that its inverse is easy to compute, or a linear system $My = c$ should be easy to solve. It is desirable that $M^{-1}A$ is as close to the identity matrix as possible. We have chosen $M$ to be the diagonal component of matrix $A$. Although this preconditioner may be inadequate for many situations, we have found it to give good results in our numerical experiments, as will be shown later. It may be noted that our choice of the preconditioner (diagonal matrix) is equivalent to the Jacobi iteration matrix. Among the other choices for preconditioners applicable to dense systems are the iteration matrices of Gauss–Seidel and successive over relaxation (SOR) schemes.

## Test Cases and Results

It is well known that wings with low thickness-to-chord ratio ($t/c$) can give rise to matrices that have predominant off-diagonal entries. This is because upper and lower panels are in close geometric proximity and hence have a strong influence on each other, but the $i$ and $j$ indices are far apart, leading to large off-diagonal elements. In subsonic panel methods that use stretching to apply linear compressibility corrections, the $t/c$ is further reduced at high subsonic Mach numbers leading to matrices with less favorable spectral properties. Therefore, to provide severe test cases, we have chosen two geometries with low $t/c$ ratios (~0.05): a delta wing (AFWAL wing[7]) and a fighter aircraft configuration. In the wing case, the panels belonging to a chordwise strip are arranged one after the other, confining the large off-diagonal entries to the corresponding block diagonal. In the aircraft case, the panels on the fuselage are not arranged in any specific order. Some of the panels are elongated and skewed. One such panel may have strong influence on a number of panels. These, along with the panels on the thin wing, have led to a poorer matrix structure in the aircraft case.

The analyses were at a high subsonic Mach number (0.7), leading to effective $t/c$ ratios in the range of 0.02–0.03. The wing case generated a 465 × 465 matrix and the aircraft configuration case a 1236 × 1236 matrix. For converged pressure distributions, upper bounds on the $L_\infty$ norms on the residuals of 0.0002 and 0.005 were found to be sufficient for the wing case and the aircraft case, respectively.

The linear systems were solved using three techniques: Gauss–Seidel iterations, conjugate gradient squared without preconditioning (CGS), and conjugate gradient squared with diagonal preconditioning (D-CGS). Figure 1 shows the comparison of the convergence

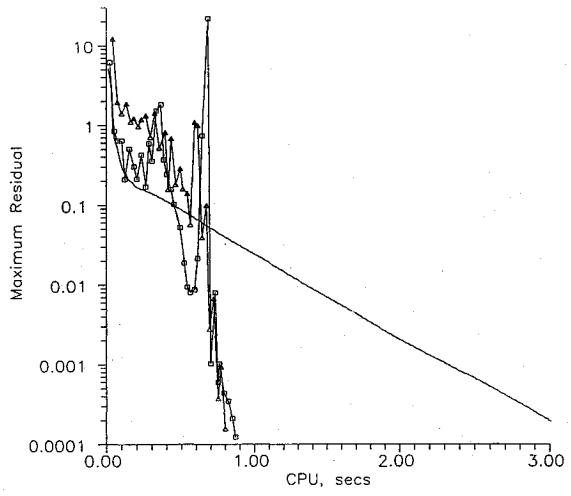


**Fig. 1 Convergence history of the three schemes for AFWAL wing analysis: ——, Gauss–Seidel; —□—, CGS; and —△—, D-CGS.**

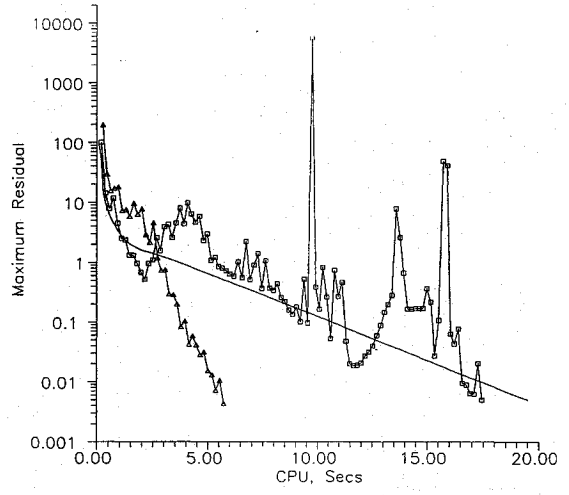


**Fig. 2 Convergence history of the three schemes for fighter aircraft configuration analysis: ——, Gauss–Seidel; —□—, CGS; and —△—, D-CGS.**

histories of the three schemes for the wing case. It may be observed that CGS and D-CGS bring down the residuals very fast. In comparison with Gauss–Seidel iterations, CGS gives a speedup of 3.5. This is good speedup considering that Krylov subspace methods are known to perform not very well without preconditioners. D-CGS is only marginally faster, with a speed up of 3.8.

Figure 2 shows the convergence histories of the three schemes for the aircraft case. Here, it may be noted that the performance of CGS is very poor. There is hardly any speedup over Gauss–Seidel relaxation; the speedup is only 1.1. Although CGS converges to the required accuracy, its convergence history is very irregular. The poorer convergence should be attributed to the poorer structure of the matrix, as explained earlier. As expected, preconditioning improves convergence. Thus D-CGS gives a speedup of 3.4. It may be noted that the convergence history is also much better behaved.

## Conclusions

The conjugate gradient squared algorithm has been implemented in the solution of subsonic potential flow problems using panel methods. The scheme gives good speedups over Gauss–Seidel iterations, of about 3.5, when it is applied to analyzing the flow past a thin wing. With diagonal preconditioning the improvement is marginal. However, when applied to analyzing the flow past a fighter configuration with irregular unstructured panels distributed on the fuselage, the scheme performs poorly without a preconditioner. Diagonal preconditioning considerably improves the convergence, giving a speedup

of about 3.4. The preconditioned conjugate gradient squared method appears to be a viable tool for improving the performance of panel codes.

## References

[1]Johnson, F. T., "A General Panel Method for the Analysis and Design of Arbitrary Configurations in Incompressible Flows," NASA CR 3079, May 1980.

[2]Sonnenveld, P., "CGS, a Fast Lanczos-Type Solver for Nonsymmetric Linear Systems," *SIAM Journal of Scientific and Statistical Computing*, Vol. 10, No. 1, 1989, pp. 36–52.

[3]Sudhakar, K., Koruthu, S. P., and Shevare, G. R., "3D Wing Analysis Using a Low Order Panel Method," *Journal of the Aeronautical Society of India*, Vol. 38, No. 4, 1986, pp. 303–306.

[4]Fletcher, R., "Conjugate Gradient Methods for Indefinite Systems," *Lecture Notes in Mathematics*, Vol. 506, Springer–Verlag, Berlin, 1976, pp. 73–89.

[5]Saad, Y., "The Lanczos Biorthogonalization Algorithm and Other Oblique Projection Methods for Solving Large Unsymmetric Systems," *SIAM Journal of Numerical Analysis*, Vol. 19, No. 3, 1982, pp. 485–506.

[6]Vitaletti, M., "Solver for Unfactored Implicit Schemes," *AIAA Journal*, Vol. 29, No. 6, 1991, pp. 1003–1005.

[7]Boersen, S. J., and Elsenaar, A., "Tests on the AFWAL 65° Delta Wing at NLR: A Study of Vortex Flow Development Between Mach = 0.4 and 4," *Proceedings of the Symposium on International Vortex Flow Experiment on Euler Code Validation* (Stockholm, Sweden), FFA, Bromma, Sweden, 1986, pp. 23–36.

# Correct Limit Approximations for Planar, Cylindrical, and Spherical Blast Waves

Qifeng Zhu,* Wataru Masuda,† and Kiyoshi Yatsui‡
*Nagaoka University of Technology, Nagaoka, Niigata 940-21, Japan*

## Introduction

THE blast wave refers to the shock-bounded flowfield produced by an energy release along a plane, a line, or at a point, which is called planar, cylindrical, and spherical blast wave, respectively. The energy is assumed to be infinitely concentrated and released instantaneously. Viscosity, thermal conductivity, real gas effects, and radiant energy losses in the flowfield behind the shock front are neglected. The flowfield ahead of the shock front is assumed to be uniform. The idealized problem of a strong explosion represents a typical example of a self-similar flow. The similarity solutions were found by Taylor[1] in connection with atomic bomb research. The first-order theory of a strong cylindrical blast wave was given by Sakurai[2] and Lin.[3] For a strong blast wave, the initial gas pressure is very small in comparison with the pressure behind the shock wave and can be neglected. This is equivalent to neglecting the initial internal energy of the gas in comparison with the explosion energy. When the shock wave becomes so weak that the initial pressure is no longer negligible compared with the pressure behind the shock, the first-order theory will be incorrect. This occurs near Mach number of 3.3 when the pressure ratio across the shock front drops below 10. The second-order theory, which gives a correction to the first-order theory for intermediate and weak waves, has been proposed by Sakurai.[4] As shown by Vlases and Jones,[5] the first-order theory fits the experimental points very well only for strong waves. However, Sakurai's second-order approximation appears to give too large a correction to the first-order theory for intermediate and weak waves. The correction term in a power series expansion in $M^{-2n}$ ($M$ is shock Mach number, $n = 1, 2, \ldots$) in Sakurai's high-order theory is slowly convergent. Based on the snowplow theory, Vlases and Jones have obtained a correct limit approximation for a cylindrical wave that predicts the shock trajectory very well down to $M = 1.16$.

It is the purpose of this paper to propose a simple method and develop the correct limit formulas to predict the shock trajectories over a wide range for planar, cylindrical, and spherical blast waves.

Received Nov. 26, 1994; revision received June 20, 1995; accepted for publication July 5, 1995. 

*Ph.D. Student, Department of Energy and Environment Science.
†Professor, Department of Mechanical Engineering.
‡Professor, Department of Electrical Engineering and Laboratory of Beam Technology.

## Brief Review of High-Order Theory and Snowplow Theory

### Sakurai's High-Order Theory

Sakurai has obtained the solution in the form

$$(1/M^2)(\bar{R}_0/R)^{\alpha+1} = J_0[1+\lambda_1(1/M)^2+(\lambda_2/2)(1/M)^4+\cdots] \quad (1)$$

where $R$ and $\bar{R}_0$ are the distance of shock front from the charge and the characteristic radius, respectively. Furthermore, $\alpha = 0, 1$, and 2 corresponds to a planar, a cylindrical, and a spherical wave, respectively, and $J_0$ and $\lambda_i (i = 1, 2, \ldots)$ are the constants. The values of $J_0$ and $\lambda_1$ have been given in Refs. 2 and 4. For example, $J_0 = 0.877$ and $\lambda_1 = -1.989$ for $\alpha = 1$ and $\gamma = 1.4$.

Sakurai has defined $\bar{R}_0$ as $(\bar{E}_\alpha/p_0)^{1/(\alpha+1)}$, where $\bar{E}_\alpha = \int_0^R [\rho u^2/2 + (p - p_0)/(\gamma - 1)]r^\alpha \, dr$, and $u$, $p$, and $\rho$ are the flow velocity, the pressure, and the density, respectively. In addition, $p_0$, $\gamma$, and $r$ are the pressure of undisturbed fluid, the ratio of specific heats, and the coordinate, respectively. In this paper, however, we alternatively define $R_0$ as $R_0 = (4E_\alpha/B\gamma p_0)^{1/(\alpha+1)}$, where for $\alpha = 0$, 1, or 2; $E_\alpha = \bar{E}_\alpha$, $2\pi\bar{E}_\alpha$, or $4\pi\bar{E}_\alpha$; and $B = J_0/\gamma$, $2\pi J_0/\gamma$, or $4\pi J_0/\gamma$, respectively. Therefore, we have $R_0 = (4\bar{E}_\alpha/p_0 J_0)^{1/(\alpha+1)} = (4/J_0)^{1/(\alpha+1)}\bar{R}_0$. Then Eq. (1) becomes

$$(1/M^2)(R_0/R)^{\alpha+1} = 4\left[1+\lambda_1(1/M)^2+(\lambda_2/2)(1/M)^4+\cdots\right] \quad (2)$$

The first-order and second-order approximations are given by Eqs. (3) and (4), respectively, as

$$(1/M^2)(R_0/R)^{\alpha+1} = 4 \quad (3)$$

$$(1/M^2)(R_0/R)^{\alpha+1} = 4\left[1 + \lambda_1(1/M)^2\right] \quad (4)$$

Integrating Eq. (4), we can obtain the following shock trajectory equation for $\gamma = 1.4$ and $\alpha = 1$:

$$\tau = 0.251\left[(1 + 7.96\lambda^2)^{\frac{1}{2}} - 1\right] \quad (5)$$

where $\lambda$ and $\tau$ are defined as $\lambda = R/R_0$ and $\tau = Ct/R_0$, and $C$ and $t$ are the sound velocity of undisturbed fluid and the time, respectively.

### Snowplow Theory

The similarity solution shows that almost all of the mass is contained within a thin layer near the front surface. In the snowplow model of Vlases and Jones, all of the mass is assumed to be concentrated in a thin layer at the shock front and travel with the shock velocity. By using this model, Vlases and Jones have obtained a simple expression for a cylindrical blast wave in the form

$$\tau = \tfrac{1}{2}\left[(1 + 4\lambda^2)^{\frac{1}{2}} - 1\right] \quad (6)$$

## Correct Limit Conditions

The correct limit condition as $\lambda \to 0$ used in Ref. 5 for a cylindrical blast wave is

$$\tau = \lambda^2 \quad (7)$$

Here, we present a general expression as the correct limit condition for $\lambda \to 0$ based on Sakurai's first-order theory, since the agreement between the theory and experiment is very good for a strong wave. Substituting $M = d\lambda/d\tau$ and $\lambda = R/R_0$ into Eq. (3) and integrating, we have

$$\tau = 4(\alpha + 3)^{-1}\lambda^{(\alpha+3)/2} \quad (8)$$